

WIND INDUCED DISPERSION AND ALGAL GROWTH IN SHALLOW LAKES

FRANCIS A. DiGIANO, LAMBERTUS LIJKLEMA and GERRIT VAN STRATEN

Department of Chemical Engineering, Twente University of Technology, Enschede (The Netherlands)

(Received 10 May 1977; revised 16 July 1977)

ABSTRACT

DiGiano, F.A., Lijklema, L. and Van Straten, G., 1978. Wind induced dispersion and algal growth in shallow lakes. *Ecol. Modelling*, 4: 237–252.

The objectives of this paper are (1) to present experimental measurements of wind induced, vertical dispersion in Lake Brielle, The Netherlands, and (2) to examine the utility of a euphotic–dark zone model for investigation of the effects of dispersion and sedimentation on algal growth and phosphate cycling in shallow lakes. A tracer technique was used to measure dispersion (D) caused by a moderate wind of 4 m/s. The resulting values ranged between 4 and 6 cm²/s and compared well with that predicted from theory. The latter objective was accomplished by comparing the results of a simple, two compartment model with those using a more complex, but more descriptive, finite difference model which accounts for the algal concentration gradient induced by growth, dispersion and sedimentation. Simulations showed good agreement in computation of the average euphotic and dark zone algal concentrations between the two models for D ranging from 0 to 6 cm²/s and for a sedimentation rate constant, K_s , of 0.002 and 0.02 m/h.

The results of simulations suggest that rapid algal growth occurs most readily in calm weather when wind induced dispersion is negligible. Dispersion may also influence the rate of particulate phosphate accumulation in the sediment (due to the settling out of algal cells) and the soluble phosphate profile in the overlying water column. Field data is needed to verify the relationship between algal growth and wind induced dispersion.

INTRODUCTION

The influence of wind action on mixing depth in deeper thermally stratified lakes has been reported by Stephan et al. (1976). Their most important finding was that several days of calm weather produced shallow mixing depths and sharp increases in epilimnic algal concentrations. Lorenzen and Mitchell (1975) have implied a similar inverse relationship between mixing depth and algal concentration for light limited growth; however, they did not consider the natural occurrence of wind action as a controlling factor. In another approach, Bella (1970) examined the effect of seasonal variations in vertical mixing caused by variations in the vertical temperature gradient. As expected, thermocline formation in the summer reduced transport of algae

by dispersion of algae to the hypolimnion and thereby caused higher epilimnic algal concentrations.

All of these studies were concerned with vertical transport in relatively deep lakes. However, wind action may also be important in shallow lakes. This is particularly true for eutrophic lakes characterized by light limited growth of algae. In these lakes, growth rate decreases sharply with depth due to the attenuation of light. Under calm conditions, sedimentation is the only physical process accounting for loss of algae from the highly productive, upper light zone. However, dispersive transport will also occur when wind action becomes significant. In addition to algal growth, other chemical cycling processes will be affected. This has been illustrated by results of a simulation model applied to Lake Brielle in southwest Netherlands (Lijklema, 1977).

The objectives of this paper are two-fold. First, experimental measurements of wind induced dispersion in Lake Brielle will be presented and compared to theoretical calculations. Secondly, the utility of a simple two compartment model, i.e. consisting of euphotic and dark zones, will be used to show the effects of dispersion and sedimentation on algal growth; these results will be compared to those predicted by a multi-layer model which more accurately accounts for concentration gradients. The ultimate goal of the research is to include the effect of wind induced mixing on the fluxes of algae and chemical species linked to the phosphate cycling process in shallow lakes.

MEASUREMENTS OF VERTICAL DISPERSION

The apparatus used for measuring vertical dispersion in Lake Brielle is shown in Fig. 1. A continuous flow of tracer solution of Rhodamine dye was

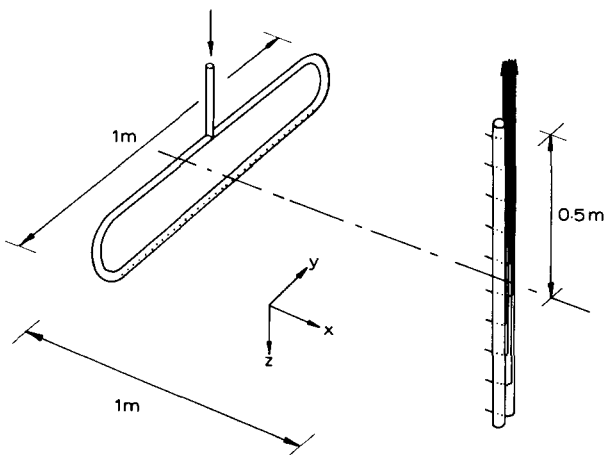


Fig. 1. Dispersion measuring apparatus.

pumped into a horizontal pipe fitted with numerous in-line holes. These holes were positioned and of a size such that the injector pipe could be considered as a uniform line source. A vertical bar was suspended a horizontal distance of 1 m from the injector and in the direction of flow. This vertical bar held ten small tubes spaced equidistantly. Each tube was connected to the surface by a sampling hose, thereby allowing for continuous sampling. Dispersion measurements were made at depths of 0.5 and 2 m. The short distance between the line source and the sampling apparatus enabled measurement of a more or less local dispersion coefficient.

The appropriate differential equation describing this measuring condition is

$$U \frac{\partial c}{\partial x} = D_z \frac{\partial^2 c}{\partial z^2}, \quad (1)$$

where U is the horizontal component of water velocity, c the dye tracer concentration, D_z the vertical dispersion coefficient and x and z , the horizontal and vertical directions, respectively. The z distance is measured with respect to the injection depth below the surface. The assumptions implicit in using Eq. (1) are:

- (i) $\frac{\partial c}{\partial t} = 0$ since the tracer stream is injected continuously;
- (ii) $\frac{\partial c}{\partial y} \sim 0$ at $y = 0$ i.e. at the center line of the dispersion plane produced by the line source;
- (iii) $D_x \frac{\partial^2 c}{\partial x^2} \ll U \frac{\partial c}{\partial x}$ i.e. dispersion in the direction of flow is neglected.

With the appropriate boundary conditions, the solution to Eq. (1) becomes

$$C(x, z) = \frac{M}{\sqrt{4\pi D_z x U}} \exp\left[\frac{-z^2 U}{4 D_z x}\right], \quad (2)$$

where M is the mass flux injected per unit of injector length and x is measured with respect to the point of injection. A plot of $\ln c(x, z)$ versus z^2 should yield a straight line with a slope of $-U/4D_z x$. With U known, D_z can be computed. A typical set of experimental results is given in Fig. 2. In this study, bottles suspended at the appropriate depth and connected to a small floating cork permitted measurement of the direction and magnitude of the velocity, U . The three calculated values of D_z are shown in Table I along with the depth and water velocity. The wind velocity during these measurements was 4 m/s and the resulting D_z ranged from 4 to 6 cm²/s. The limited number of measurements and the lack of precision of the experimental technique prevent conclusions being reached regarding the dependence of D_z on depth.

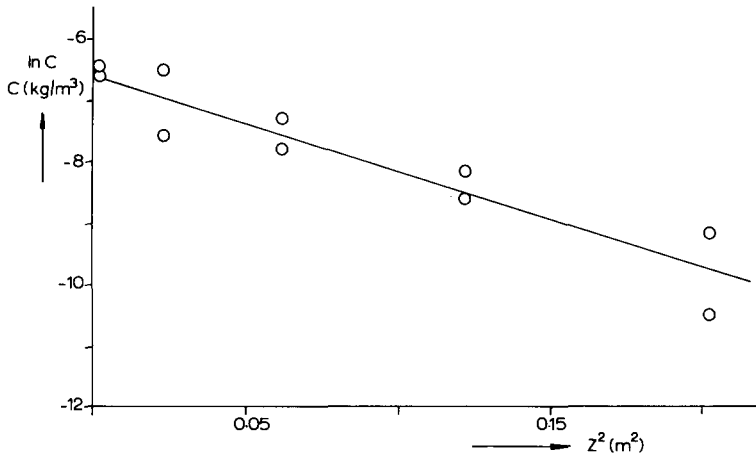


Fig. 2. Typical results of dispersion measurements.

These experimental results can be compared to those predicted from theory. Banks (1975) has presented a summary of the literature in this field and gives the relationship between vertical eddy viscosity, ϵ_z , and wind velocity, W , and water depth, H , as

$$\epsilon_z = \frac{1}{4} \frac{\rho_a}{\rho} \frac{c_z}{\alpha} HW. \quad (3)$$

In Eq. (3), ρ_a is the density of air and ρ the density of water; c_z , the wind stress coefficient, is determined by the relationship between shear stress, τ_s , at the water surface and the wind velocity as given in Eq. (4):

$$\tau_s = c_z \rho_a W^2. \quad (4)$$

The term α in Eq. (3) represents the ratio between surface water velocity, U_s , and wind velocity W (as measured at a distance of 10 m above the water

TABLE I
Measured dispersion coefficients
Wind velocity = 4 m/s

Depth (m)	U (m/s)	$-U/4D_zX$	D_z (cm ² /s)
0.5	~0.035	15	6
0.5	~0.035	21	4
2.0	~0.03	15	5

surface)

$$U_s = \alpha W. \quad (5)$$

Eq. (3) is based on the Boussinesq eddy diffusivity concept of turbulent flow. Although oversimplified, this theory is still appropriate for the present analysis. It should be recognized that both c_z and α relate to the wind path length over the lake surface and must therefore be evaluated for each individual lake. For Lake Brielle, $c_z \sim 1 \times 10^{-3}$, $\alpha = 0.02$ and $H = 10$ m (at the measuring site) are reasonable values. Thus, the vertical eddy diffusivity is related to wind velocity (m/s) by

$$\epsilon_z \text{ (m}^2\text{/s)} \sim 1.5 \times 10^{-4} W. \quad (6)$$

Assuming that the Reynolds analogy is justified, this relationship predicts D_z values which compare well to those measured.

ALGAL GROWTH MODELS

Algal concentration in the euphotic zone is determined by the rates of algal growth and mineralization along with sedimentation and dispersion. The appropriate mass balance is:

$$\frac{\partial A}{\partial t} = A_G(t) - A_D(t) + D_z \frac{\partial^2 A}{\partial z^2} - K_s \frac{\partial A}{\partial z}, \quad (7)$$

where A is the algal concentration, $A_G(t)$ and $A_D(t)$ the algal growth and mineralization rates, respectively, D_z , the dispersion coefficient, K_s , the sedimentation coefficient and z , the vertical distance. The cross sectional area is assumed uniform with depth and sedimentation is described in terms of the net flux across upper and lower boundaries of the volume element. Similarly, the mass balance accounting for algal death, sedimentation and dispersion in the dark zone is given by:

$$\frac{\partial A}{\partial t} = -A_D(t) + D_z \frac{\partial^2 A}{\partial z^2} - K_s \frac{\partial A}{\partial z}. \quad (8)$$

The distribution of soluble phosphate is affected by algal growth dynamics and by dispersion. For the euphotic zone, a phosphate balance yields

$$\frac{\partial P}{\partial t} = D_z \frac{\partial^2 P}{\partial z^2} - Y_P A_G(t) + Y_P A_D(t), \quad (9)$$

in which Y_P is the stoichiometric amount of phosphate either incorporated into an algal cell during growth or released by death of the cell. Hence, complete recycling of phosphate upon death of algae has been assumed. There is

no phosphate uptake associated with the dark zone and thus,

$$\frac{\partial P}{\partial t} = D_z \frac{\partial^2 P}{\partial z^2} + Y_P A_D(t). \quad (10)$$

The equation developed by Smith (1936) can be used to describe light limited, algal growth as

$$A_G(t) = \mu_{\max} \left[\frac{I(t)/I_K}{\sqrt{1 + (I(t)/I_K)^2}} \right] A, \quad (11)$$

where μ_{\max} is the maximum specific growth rate, $I(t)$, the light intensity at any depth z , and I_K , a constant defining the light dependency. The main objective of modelling in this research was to examine the effect of wind induced mixing on growth; thus, growth limitation by phosphate was not included. In addition, the present condition of Lake Brielle is that of light limited rather than phosphate limited growth. Attenuation of light with depth becomes an important factor in generating the vertical algal concentration profile and thus in influencing the dispersive and sedimentation fluxes. Beer's law has been applied to describe the extinction of light in lake water as

$$I(t) = I_0(t) \exp[-Ez], \quad (12)$$

where $I_0(t)$ is the intensity of light at the surface and E is the attenuation coefficient given by

$$E = a + bA. \quad (13)$$

In Eq. (13), a is the light extinction coefficient for the lake water itself and b the coefficient associated with light extinction caused by algae. A sinusoidal pattern for I_0 as a function of time (i.e. from 06.00 to 18.00 h) is assumed.

A simple, first-order relationship for algal mineralization rate is given by

$$A_D(t) = -K_d A, \quad (14)$$

in which K_d is the mineralization rate coefficient. The net specific growth rate term $[A_G(t) - A_D(t)]/A$, as presented in Fig. 3, is thus a function of the daily light cycle and of depth within the euphotic zone. The rapid decline in net specific growth rate with depth also suggests a steep algal concentration gradient, especially during the period of maximum light intensity.

The highly non-linear dependency of algal growth on time and depth shown in Fig. 3 precludes the use of an analytical solution to Eqs. (7) and (8). Two modelling alternatives are therefore presented: (1) a finite difference scheme and (2) a simpler, two compartment scheme consisting of the euphotic and dark zones.

In the finite difference model, the obvious boundary condition at the sur-

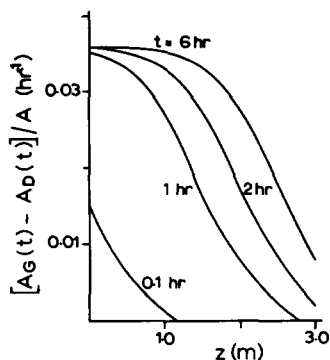


Fig. 3. Light limited net specific growth rate in euphotic zone and time after sunrise as a function of depth.

$$I_{0\max} = 0.4 \text{ cal/cm}^2/\text{min}; I_k = 0.02 \text{ cal/cm}^2/\text{min};$$

$$E = 1.4 \text{ m}^{-1}; \mu_{\max} = 0.04 \text{ h}^{-1}; K_d = 0.004 \text{ h}^{-1}.$$

Note: Growth is over a 12 h light cycle with the maximum rate at 6 h.

face of the water is that no material is lost to the atmosphere. At the lower boundary (i.e. at the sediment-water interface), the following boundary condition was used:

$$D_z \frac{\partial^2 A}{\partial z^2} = 0 \quad (15)$$

In a physical sense, the boundary condition given by Eq. (15) is reasonable because the element lying just above the sediment can be considered as a viscous sub-layer in which only sedimentation of algae occurs.

In the two compartment model, algal growth in the euphotic zone is averaged by integrating Eq. (11) over the euphotic depth, i.e. over Z_e , such that

$$A_G(t) = \frac{\mu_{\max} A_e}{E Z_e} \ln \left[\frac{\frac{I_0}{I_K} + \sqrt{1 + \left(\frac{I_0}{I_K}\right)^2}}{\frac{I_{Z_e}}{I_K} + \sqrt{1 + \left(\frac{I_{Z_e}}{I_K}\right)^2}} \right], \quad (16)$$

where A_e is the algal concentration in the euphotic zone, I_{Z_e} is the light intensity at the lower limit of the euphotic zone and the other symbols are as previously defined.

Accordingly, algal mineralization rate is given by

$$A_D(t) = K_d A_e. \quad (17)$$

The rate of change of algal concentration by dispersion is approximated by

$$\frac{D_z}{(Z_e)^2} [A_e - A_d], \quad (18)$$

and by sedimentation by

$$\frac{K_s}{Z_e} [A_e - A_d], \quad (19)$$

where A_d is the algal concentration in the dark zone.

The corresponding terms describing dark zone processes are as follows:

$$A_d(t) = K_d A_d, \quad (20)$$

$$\frac{D_z}{(Z_d)^2} [A_e - A_d], \quad (21)$$

$$\frac{K_s}{Z_d} A_d, \quad (22)$$

in which Z_d is the depth of the dark zone.

SIMULATION APPROACH

The finite difference model yields the complete algal concentration profile over the depth of the water column as a result of substituting the appropriate differential rate terms given by Eqs. (11), (12) and (14) into the mass balances given by Eqs. (7) and (8). It should be noted that the computational scheme for this model has been simplified by first averaging the algal concentrations generated in the euphotic zone to obtain an average value of the light extinction coefficient, E (see Eq. (12)). The two compartment model can only provide algal concentration in the euphotic and dark zones by substituting Eqs. (16)–(19) into Eq. (7) and Eqs. (20)–(22) into Eq. (8). A similar distinction in approach between the two models exists for calculation of phosphate concentrations.

The primary objective of simulations was to determine if the simple two-compartment model was sufficient to describe the effects of dispersion on algal growth dynamics.

Thus, algal concentration–depth profiles generated by the finite difference model for a range of dispersion coefficients were averaged for the euphotic and dark zones and then compared to those computed by the two compartment model. Results of the finite difference model were also of importance in examining the effect of dispersion and sedimentation on the shapes of the algal and phosphate concentration profiles and on the flux of algae to the sediment.

TABLE II
Input data for simulations

Total depth	5 m
Euphotic depth	2.5 m
μ_{\max}	0.04 h ⁻¹
K_d	0.004 h ⁻¹
$I_{0\max}$	0.4 cal/cm ² /min
I_K	0.02 cal/cm ² /min
a	1.0 m ⁻¹
b	0.25 m ⁻¹ mg ⁻¹ l
Y_P	0.0128 mg P/mg dry weight algae *
A_0	1.6 mg/l
P_0	50 μ g/l as P
D	0, 1, 2 and 6 cm ² /s
K_s	0.002 and 0.02 m/h

* Based upon a molecular formula for algae of C₁₀₆H₁₈₁O₄₅N₁₆P.

Table II lists the input data required for simulations and the values of D and K_s selected for study. The choice of a total depth of 5 m and euphotic zone depth of 2.5 m were consistent with the physical features of Lake Brielle, and shallow lakes in general. The depth of the euphotic zone can be seen from Fig. 3 to vary throughout the day. This depth is also affected by the algal concentration due to its relationship to light attenuation (see Eq. (12)). The selection of 2.5 m in this case is an approximation to the maximum euphotic depth for low algal concentrations and maximum light intensity. Use of a maximum depth in the multi-layer model assures calculation of algal growth at lower depths during peak light intensity periods. With lower light intensities, growth is negligible at these lower depths. Selection of μ_{\max} , K_d and the light extinction parameters I_0 , I_k , a , and b was not entirely based on Lake Brielle data; rather, these values were considered reasonable estimates for comparison of simulation results in which the dispersion coefficient was the main parameter of concern. The initial phosphate concentration of 50 μ g/l P represents only the soluble fraction. This value is much less than that presently found in Lake Brielle (generally ranging from 100 to 300 μ g/l); however, use of a lower concentration in simulations better illustrated the effect of algal growth dynamics on the phosphate profile by producing a larger incremental change in phosphate concentration.

Field measurements, as described herein, were used to select the range of dispersion coefficients for simulations. There are no known field measurements of K_s in Lake Brielle. Thus, a range of values suggested from literature (Imboden, 1974) provided a basis for testing the importance of this parameter in modelling algal growth.

SIMULATION RESULTS

The THT-SIM, a conversational simulation language, was used for simulations. To minimize computation time, only ten elements were used in the finite difference model. Tests with more elements gave similar results. The time step was always 0.05 h or less.

Figs. 4 a and b show the algal concentration—depth profiles obtained in the finite difference model at $t = 60$ h for $D = 0$ and $1 \text{ cm}^2/\text{s}$, respectively.

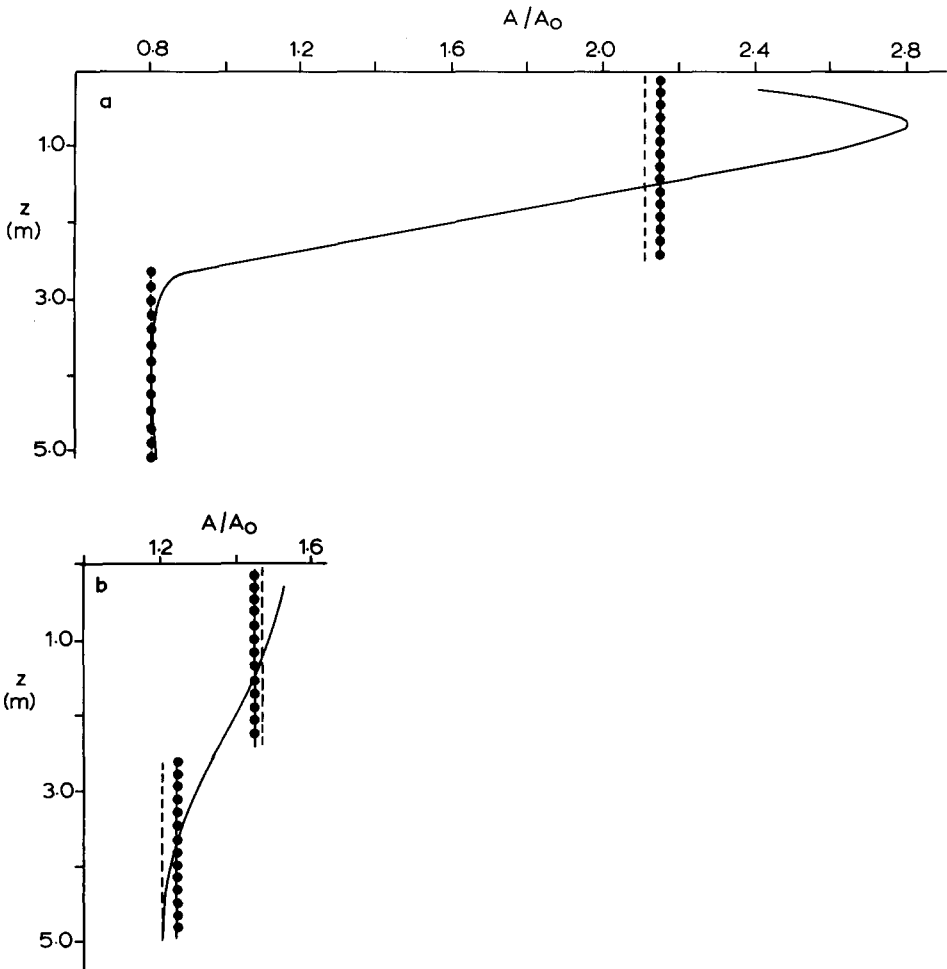


Fig. 4. a: Algal profile after 60 h in the absence of dispersion, i.e. $D = 0 \text{ cm}^2/\text{s}$. b: Influence of dispersion on algal profile after 60 h. $D = 1 \text{ cm}^2/\text{s}$. — Ten-compartment model; ●—● average euphotic and dark zone concentrations from ten-compartment model; - - - euphotic and dark zone concentrations A_e and A_d , respectively from two-compartment model. $K_s = 0.002 \text{ m/h}$.

Algal concentrations have been normalized by the initial algal concentration A_0 . A time of 60 h was selected for comparisons in order to emphasize the algal profile at maximum light intensity, i.e. the 12th h of the 3rd day of simulation; at this time algal growth rate is also a maximum.

During the night, algal concentration decreases in the euphotic zone due to algal mineralization, sedimentation and dispersion (when $D > 0 \text{ cm}^2/\text{s}$). Also shown in Figs. 4 a and b are the average concentrations in the euphotic and dark zones as computed from the finite difference model and from the two compartment model.

The importance of dispersion in determining the algal profile can best be seen by examination of the results from the finite difference model. Despite the low value of dispersion coefficient selected, algal production is greatly reduced over that for a stagnant system, i.e. $D = 0 \text{ cm}^2/\text{s}$. This is caused by dispersion of algae to lower depths as a result of the concentration gradient produced by the depth-dependent, light limited growth function given in Fig. 3. Further, the finite difference and two compartment models yielded quite comparable average algal concentrations in the euphotic and dark zones. Good agreement should have been expected in the case of $D = 0 \text{ cm}^2/\text{s}$ because, in this instance, the only difference between these models is use of the differential vis à vis the integral form of the algal growth rate expression. The fact that good agreement persists when dispersion is included suggests that averaging the algal concentration in the euphotic zone is a valid approximation for calculation of flux across the euphotic—dark zone interface.

Figs. 5 a and b show that the finite difference and two compartment models are also in good agreement for the higher value of sedimentation rate. A comparison of Figs. 4 a and b with Figs. 5 a and b provides evidence of the importance of K_s in modelling algal profiles. For $D = 0 \text{ cm}^2/\text{s}$, increasing K_s from 0.002 to 0.02 m/h produces a much lower maximum algal concentration which is located at a lower depth. A point of maximum concentration is explained by the competitive effect of growth and sedimentation rates. Thus, at higher sedimentation rates, algae are rapidly settling out of the region of maximum light intensity; but despite more severe light limitations at lower depths, a higher algal growth rate is possible due to the larger mass of algae supplied by sedimentation. Similar observations were made by Bella (1970) in discussing the importance of sedimentation of algae in thermally stratified lakes.

Good agreement was also obtained in comparing A_e from the two compartment model with the averaged euphotic zone concentration from the finite difference model over a 240-h simulation period as is shown in Fig. 6 a for $D = 1 \text{ cm}^2/\text{s}$. Thus having established the validity of the two compartment model, the effects of dispersion and sedimentation on algal growth can be examined over this extended time period. When, as shown in Fig. 6 a, a low value of K_s (0.002 m/h) is assumed and dispersion is absent, a 400% increase in algal concentration in the euphotic zone and a 160% increase in total algal mass in the water column is noted over 10 days. However, with

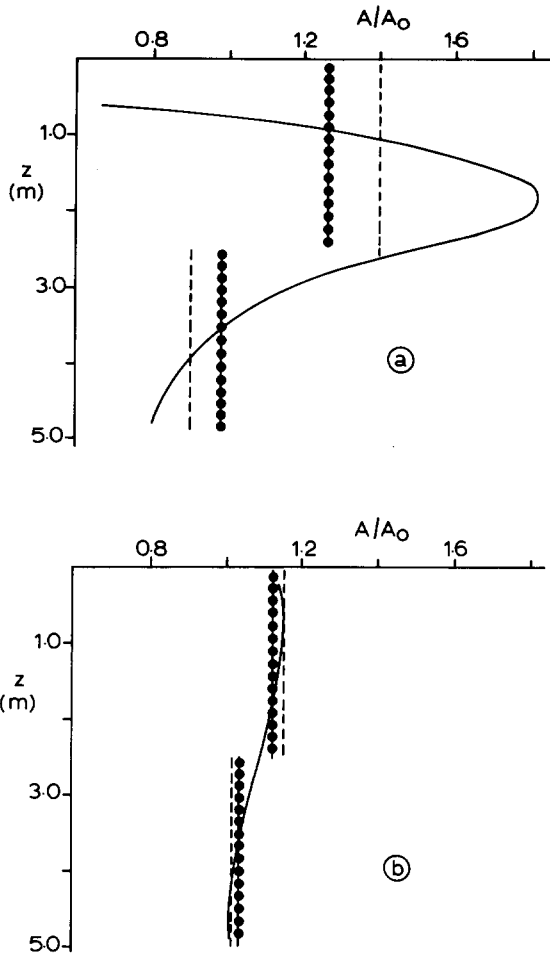


Fig. 5. Influence of dispersion on algal profile after 60 h.
 a: $D = 0 \text{ cm}^2/\text{s}$ and b: $D = 1 \text{ cm}^2/\text{s}$.
 —; ●—●—●; - - - - -; same as in Fig. 4. $K_s = 0.02 \text{ m/h}$.

inclusion of a relatively low dispersion coefficient of $1 \text{ cm}^2/\text{s}$, algal concentration in the euphotic zone, and similarly total mass in the water column, only increase by 100%. Little further attenuation of algal growth occurs with increased dispersion. These simulations suggest that intense algal growth is associated with strictly calm weather which produces little mixing action by the wind; however, only a light wind, i.e. enough to produce a D of $1 \text{ cm}^2/\text{s}$, can reduce algal growth. The substantial difference in algal growth between $D = 0$ and $1 \text{ cm}^2/\text{s}$ suggests that future research on dispersion should focus on this rather narrow region of mixing conditions.

The importance of the assumption of K_s in reaching conclusions regarding

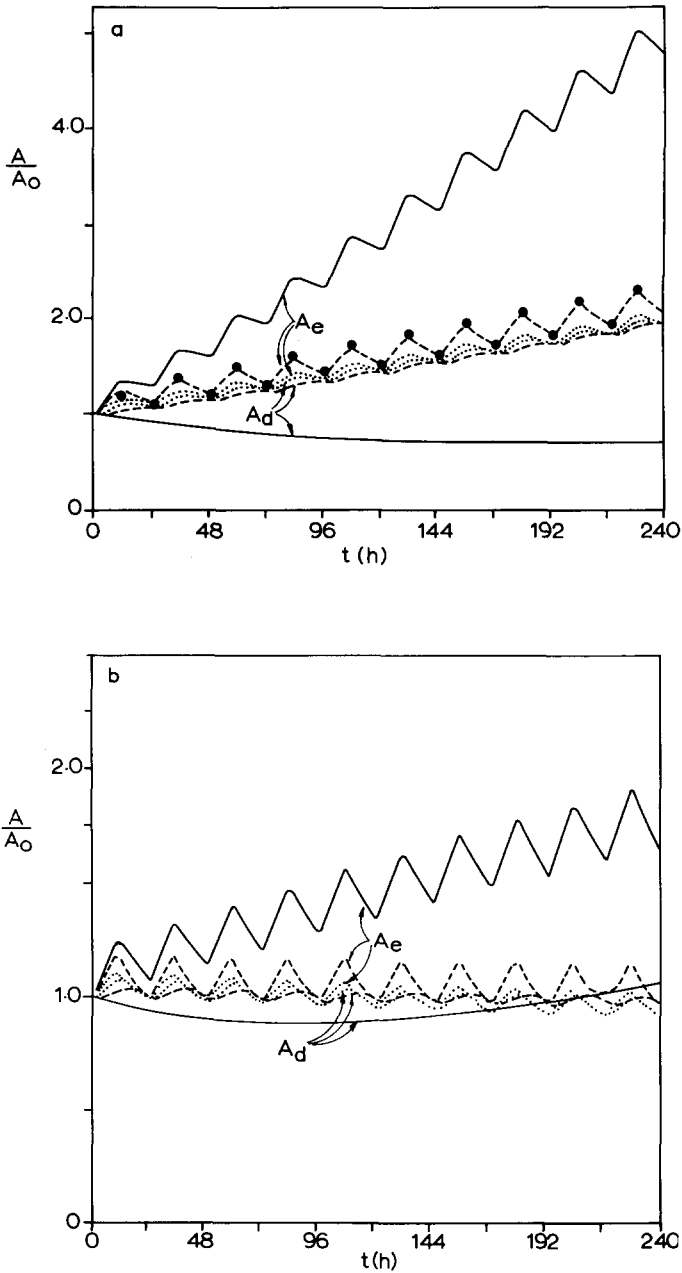


Fig. 6. Influence of dispersion on algal growth with :
 a: $K_s = 0.002$ m/h and b: $K_s = 0.02$ m/h.
 Two-compartment model results: — $D = 0$ cm²/s, - - - $D = 1$ cm²/s, $D = 6$ cm²/s.
 Averaged euphotic zone algal concentration from ten-compartment model ●●●.

the effects of dispersion is seen by comparison of Figs. 6 a and b. Fig. 6 b shows that with a higher K_s (0.02 m/h), algal growth is greatly reduced. Moreover, in these simulations, the combined effect of dispersion and a high sedimentation rate is to suppress the algal growth almost completely.

The sedimentation rate of algae in the dark zone (Eq. (22)) can be used to predict the particulate phosphorus reaching the sediment in the form of algal cells. The accumulative amount of phosphorus depends directly upon A_d as shown below:

$$P_{acc} = \int_0^t K_s Y_p A_d dt \quad (23)$$

From Fig. 6 a, the effect of dispersion is to steadily increase A_d with time; thus, the rate of phosphorus accumulation will reflect this pattern. Without dispersion, A_d decreases slightly due to the mineralization of algal cells and thereby retards the rate of phosphorus accumulation. When K_s is increased by a factor of ten, i.e. from 0.002 to 0.02 m/h, Eq. (23) predicts a nearly proportional increase in P_{acc} .

The effects of dispersion on the soluble phosphate concentration profile as generated by the finite difference model is given in Fig. 7. After simulating 60 h of algal growth, only a slight phosphate gradient exists when $D = 1 \text{ cm}^2/\text{s}$. In contrast, the higher growth rate and lack of redistribution of phosphate from the lower depths when $D = 0 \text{ cm}^2/\text{s}$ produces a very sharp gradient in the euphotic zone. Although not included in this model, lower phosphate concentration in the euphotic zone would also limit algal growth

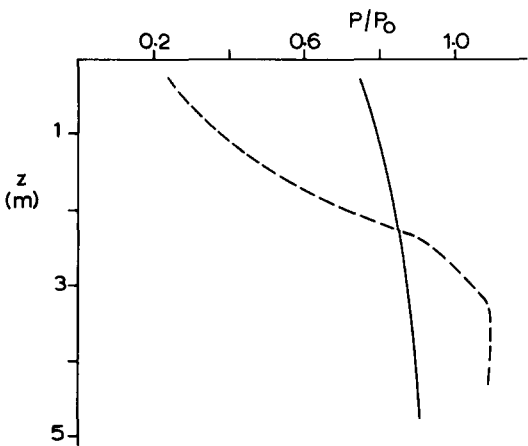


Fig. 7. Influence of dispersion on the vertical distribution of soluble phosphate after 60 h with initial soluble phosphate = $50 \mu\text{g}/\text{l}$ and $K_s = 0.002 \text{ m}/\text{h}$.
 - - - - - $D = 0 \text{ cm}^2/\text{s}$; ——— $D = 1 \text{ cm}^2/\text{s}$.

and thereby retard further the steepening of the phosphate gradient. Thus, in lakes with lower phosphate concentrations than in Lake Brielle, a secondary and opposite effect of the absence of dispersion could be a development of a nutrient limited, algal growth situation. This effect would lessen the difference between algal growth predicted for $D = 0$ and $1 \text{ cm}^2/\text{s}$ under only light limiting growth conditions.

CONCLUSIONS

Vertical dispersion coefficients measured by a tracer technique compared well to values derived from theory. In Lake Brielle, typical values for moderate winds (4 m/s) ranged over $4\text{--}6 \text{ cm}^2/\text{s}$.

The effects of dispersion and sedimentation were conveniently included in a simple, two compartment model of algal growth in shallow lakes. Simulation results indicated good agreement between this model and the more precise, finite difference model. Wind induced dispersion which produces a D value of only $1 \text{ cm}^2/\text{s}$ greatly suppressed growth in the euphotic zone over a simulation period of 10 days. However, little more attenuation of growth occurred when the dispersion coefficient was increased further. A question remains as to whether or not values close to $D = 0 \text{ cm}^2/\text{s}$ actually occur during calm weather, since thermal processes can cause density gradients which may induce vertical transport.

The assumed sedimentation constant, K_s , also influenced the extent of algal growth. A higher sedimentation constant caused more restricted growth; this was even more pronounced when the effect of dispersion was included. Sedimentation and dispersion also interacted to determine the rate of particulate phosphorus accumulation, P_{acc} , in the sediment. Increased dispersion actually increased this rate due to the effect of increasing the dark zone algal concentration. Model simulations indicated that dispersion also influences the phosphate profile in the water column. Thus, dispersion can affect algal growth rate in lakes in which phosphate is the limiting nutrient.

These simulations have thus shown that dispersion may play an important role in the phosphate cycling processes in shallow lakes by altering the algal growth pattern and the rate of phosphate accumulation in the sediment. However, the stochastic nature of wind induced dispersion remains to be considered in modelling. Long periods of either complete calm or steady wind are very unlikely. In this regard, field correlations between wind velocity and algal productivity are needed along with more extensive measurements of particulate sedimentation rates.

ACKNOWLEDGEMENTS

The authors are grateful to the Environmental Division of the Deltadienst, Rijkswaterstaat for their cooperation and to Ir. G.J. Roskam, who contributed in the field measurements.

REFERENCES

- Banks, R.B., 1975. Some features of wind action on shallow lakes. *J. Environ. Eng. Div. Am. Soc. Civ. Eng.*, 101 (EE5): 813–827.
- Bella, D.A., 1970. Simulating the effect of sinking and vertical mixing on algal population dynamics. *J. Water Pollut. Control Fed.*, 42(5): R140–R152.
- Imboden, D.M., 1974. Phosphorus model of lake eutrophication. *Limnol. Oceanogr.*, 19 (2): 297–304.
- Lijklema, L., 1977. The role of iron in the exchange of phosphate between water and sediments. In: *Proc. S.I. L.—UNESCO Symposium — Interactions between Sediments and Freshwater*, Amsterdam, 6–10 September 1976. Pudoc, Wageningen, pp. 313–317.
- Lorenzen, M.W. and Mitchell, R., 1975. An evaluation of artificial destratification. *J. Am. Water Works Assoc.*, 67: 373–376.
- Smith, E.L., 1936. Photosynthesis in relation to light and carbon dioxide. *Natl. Acad. Sci. U.S.A.*, Washington, D.C., 22: 504–510.
- Stephan, H., Skoglund, T. and Megard, R.O., 1976. Wind control of algae growth in eutrophic lakes. *J. Environ. Eng. Div. Am. Soc. Civ. Eng.*, 102 (EE6): 1201–1213.